Structural Characterization of Electron-Beam Crosslinked Thermoplastic Elastomeric Films from Blends of Polyethylene and Ethylene-Vinyl Acetate Copolymers

S. CHATTOPADHYAY, T. K. CHAKI, ANIL K. BHOWMICK

Rubber Technology Center, Indian Institute of Technology, Kharagpur-721302, India

Received 31 August 2000; accepted 9 October 2000

ABSTRACT: Films were prepared from a blend of low-density polyethylene (LDPE) and ethylene-vinyl acetate (EVA) containing 45% VA and ditrimethylol propane tetraacrylate (DTMPTA). Electron-beam initiated crosslinking of these films was carried out over a range of radiation doses (20–500 kGy), concentrations of DTMPTA (1–5 parts by weight), and blend compositions. The IR studies revealed that oxidation and crosslinking dominated up to an irradiation dose of 100 kGy. At higher irradiation doses chain scission and disproportionation predominated among all the competitive processes for the 50:50 blend without DTMPTA. The gel fraction of the films increased with the increase in irradiation dose, DTMPTA level, and EVA content of the blends. X-ray diffraction and differential scanning calorimetry studies showed that the crystalline portion of the blends was only affected by radiation at higher irradiation doses ($\geq$200 kGy). Scanning electron microscopy studies indicated that in the 50:50 blend the LDPE formed the continuous phase, which was further confirmed by atomic force microscopy and transmission electron microscopy studies. However, a co-continuous morphology was formed when the EVA content was increased. When DTMPTA was added to the blends ($\geq$3 wt %), the 50:50 blend exhibited a co-continuous morphology. © 2001 John Wiley & Sons, Inc. J Appl Polym Sci 81: 1936–1950, 2001

Key words: low-density polyethylene; ethylene-vinyl acetate; ditrimethylol propane tetraacrylate; thermoplastic elastomer; electron-beam irradiation; gel fraction; crosslinking; scission; disproportionation; morphology

INTRODUCTION

Modification of polymers and polymer blends in the presence of radiation is a potential method for the development of materials with superior properties. Electron-beam modification of polymers results in the formation of a 3-dimensional network structure through the union of *in situ* generated macroradicals.[1–3] Polyfunctional monomers, such as multifunctional acrylate and allylic reactive molecules, blended with the base polymers help to achieve crosslinking at a reduced radiation level without a significant deterioration of the base polymers.[4,5]

Electron-beam modification has certain advantages over conventional grafting processes such as the absence of catalyst residue, complete control of the temperature, it is a solvent-free system, and it is a source of enormous amounts of radicals and ions with single control and accurate reproducibility.[6–9]

Correspondence to: A. K. Bhowmick (anilkb@rtc.iitkgp.ernet.in).

Contract grant sponsor: Radiation Processing Section, Bhabha Atomic Research Centre, Mumbai.

Journal of Applied Polymer Science, Vol. 81, 1936–1950 (2001)

Blending is an effective method of modifying the properties of polymers because it is a simple operation and has low costs. Radiation crosslinking can make effective modifications of polymer blends.[10] However, use of electron-beam radiation is relatively new. This may be particularly interesting for thermoplastic elastomers from blends of rubbers and plastics, which are extensively reported.[11–15]

Different authors reviewed the treatment of polymers and polymer blends by electron-beam irradiation. It was observed that some polymers like natural rubber and ethylene propylene rubber can generally be crosslinked using electron-beam radiation,[16–19] whereas some others like polypropylene and poly(vinyl chloride) have a tendency to degrade.[20] The effects of electron-beam radiation on the structures and properties of various polymers, including polyethylene (PE) and ethylene-vinyl acetate (EVA), in the presence of different types of polyfunctional monomers were also reported by Bhowmick et al.[17,19,21–23] Martinez-Padro and Vera-Graziano carried out γ-radiation induced crosslinking of PE and EVA (18% VA content) blends.[24] Possible chemical reactions and alternative irradiation methods were also discussed. Abdel-Bary and El-Naser studied the characterization and possible application of grafted acrylamide onto low-density PE (LDPE), EVA, and their blends.[25] The influence of electron-beam irradiation on the mechanical properties of polypropylene–ethylene-propylene-diene monomer rubber blends was studied by Harnischfiger et al.[26] Mateev and Karageorgier studied the effect of electron-beam irradiation and the content of EVA (13% VA content) upon the gel forming processes in LDPE-EVA films.[27] The above authors did not report on the detailed characterization and thermoplastic elastomeric behavior of these blends. Recently, Chattopadhyay et al. discussed the heat shrinkability and mechanical properties of thermoplastic elastomeric films from blends of PE and EVA.[28,29]

The objective of the present work is to characterize thermoplastic elastomeric films from a LDPE and EVA (45% VA content) blend with variations in the radiation dose, monomer level, and blend ratio. Ditrimethylol propane tetraacrylate (DTMPTA), a tetrafunctional unsaturated monomer, was used to produce high yield of radicals during irradiation. IR spectroscopy, X-ray diffraction (XRD), and differential scanning calorimetry (DSC) measurements were used for characterization of the modified polymers. Gel fraction studies were performed to evaluate the extent of crosslinking.

EXPERIMENTAL

Materials

The EVA copolymer (Levaprene 450, 45% VA content, 0.975 g/cm^3 density, 0.26% ash content at 950°C, 0.6% maximum volatility) was supplied by Bayer, Germany. The LDPE was procured from IPCL (Indothene 16MA400, 0.918 g/cm^3 density, 3 dg/min melt index, Baroda, India). The DTMPTA (Ebecryl 140) used as the radiation sensitizer was obtained from UCB Chemicals.

Preparation of Samples

The EVA, PE, and DTMPTA were mixed in a Brabander Plasticorder (PLE-330) at 130°C with a 60 rpm rotor speed. The PE was first allowed to melt for 2 min, followed by EVA and DTMPTA, and the total mixing time was 4 min. The mixes so obtained were sheeted out through an open mill set at a 2-mm nip gap. Then they were remixed in the Brabander Plasticorder for another 2 min at 130°C.

The sheets were compression molded between Teflon sheets for 2 min at 150°C and a pressure of 5 MPa in an electrically heated press to obtain films of 0.025 $\pm$ 0.003 cm thickness. The moldings were cooled under compression to maintain the overall dimensional stability.

Our initial studies[28,29] indicated that 50:50 (w/w) EVA and PE blend irradiated in an electron beam gave rise to thermoplastic–elastomeric properties. The DTMPTA level was varied only with that composition to see the effect of the sensitizer on the properties of the blend. The blend ratio of PE and EVA was varied in another set of experiments.

Irradiation of Samples

The molded films were irradiated in air at a room temperature of 25 $\pm$ 2°C by using an electron-beam accelerator (model ILU-6) under forced air cooling at the Bhabha Atomic Research Centre (Bombay, India). Irradiation doses of 20, 50, 100, 200, and 500 kGy were used. The specifications of the electron-beam accelerator were given in earlier communications.[21–23] The formulations of the samples are given in Table I.

Table I Formulation of Samples

Sample Code	PE (wt %)	EVA (wt %)	DTMPTA (wt %)	Radiation Dose (kGy)
PE100	100	0	0	100
PEVA 55000	50	50	0	00
PEVA 55020	50	50	0	20
PEVA 55050	50	50	0	50
PEVA 55100	50	50	0	100
PEVA 55200	50	50	0	200
PEVA 55500	50	50	0	500
PEVA 55101	50	50	1	100
PEVA 55103	50	50	3	100
PEVA 55105	50	50	5	100
PEVA 37100	30	70	0	100
PEVA 37000	30	70	0	00
PEVA 46100	40	60	0	100
PEVA 64100	60	40	0	100
PEVA 73100	70	30	0	100
PEVA 73000	70	30	0	00
PEVA 55023	50	50	3	20
EVA 100	0	100	0	100

Measurement of Properties

Gel Fraction

The gel fraction was measured gravimetrically by immersing the samples in xylene at 80°C for 72 h. The equilibrium swelling time was determined from the experiments and calculated from the weight of the sample before and after swelling as follows:

$$\text{gel fraction} = w_2/w_1 \tag{1}$$

where w_1 is the initial weight of the film and w_2 is the weight of the insoluble portion of the film. The results reported here were the average of three samples.

XRD Analysis

The XRD patterns of the control, stretched, and shrunk samples were recorded with a Philips X-ray diffractometer (PW-1840) using crystal monochromated Co Kα radiation in the angular range of 10–40° (2θ) and at a 40-kV operating voltage and a 20-mA current.

The areas under the crystalline and amorphous portions were determined in arbitrary units and the degree of crystallinity (χ_c) was measured using the relation:

$$\chi_c = \frac{I_c}{I_c + I_a} \tag{2}$$

where I_a and I_c are the integrated intensity corresponding to the amorphous and crystalline phases, respectively.[30] The 2θ values could be reproduced within $\pm 0.02°$ variation.

The crystallite size (P), interchain distance (r), and interplanar distance (d) were calculated as follows:

$$P = \frac{92.26}{\beta \cos\theta} \quad (\lambda = 1.79\,\text{Å}) \tag{3}$$

$$r = \frac{5}{8}\frac{\lambda}{\sin\theta} \tag{4}$$

$$d = \frac{\lambda}{2\sin\theta} \tag{5}$$

where β is the half-height width of the crystalline peak and λ is the wavelength of the X-ray radiation. The results reported here were based on three samples.

IR Studies

IR spectra were taken on the thin films (~100 μm) using a Perkin–Elmer (model 837) spectrophotometer. The absorbance peak area was measured under a particular peak for a constant thickness of the film.

DSC Studies

DSC studies were carried out using a DuPont 9000 thermal analyzer at a heating rate of 20°C min^{-1} in nitrogen in a temperature range of −150 to 150°C. The peak minima from the melting thermogram was considered as the melting point (T_m).

The crystallinity (x_c) was calculated from the heat of fusion, which is the area of the melting peak, using the relation[31]

$$x_C = \frac{\Delta H_m}{\Delta H_c} \times 100 \tag{6}$$

where ΔH_m is the melting enthalpy of the sample and ΔH_c is the melting enthalpy of a perfectly crystalline PE sample (66.4 mcal mg^{-1}).

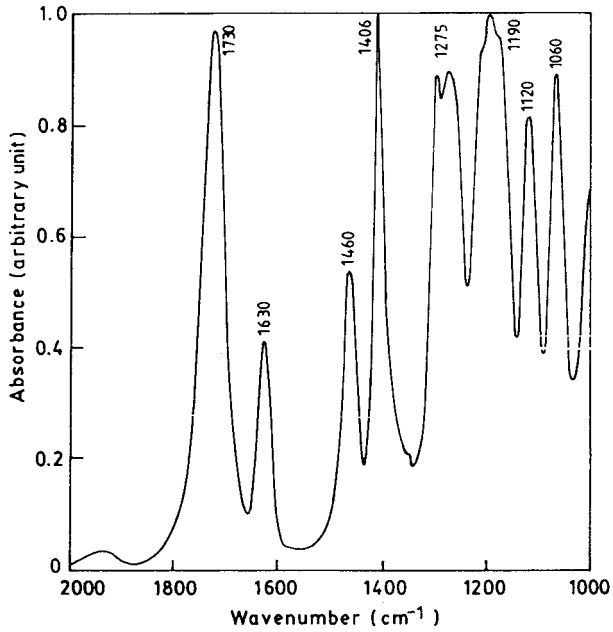

Figure 1 The IR spectra of DTMPTA in the range of 2000–1000 cm^{-1}.

Microscopy Studies

Scanning electron microscopy (SEM) photographs of the blends were taken with a JSM 5800 microscope (Jeol). The accelerating voltage was 15 kV. The EVA phase was etched out with toluene for uncrosslinked samples and concentrated nitric acid was used for crosslinked samples. The samples were gold coated prior to the SEM studies. An atomic force microscopy (AFM) image of the film was recorded in air at 25°C with a Nanoscope III (Dimension Zero, Digital Instruments Inc.) in the tapping mode using microfabricated cantilevers. For transmission electron microscopy (TEM) observation the EVA phase was stained with osmium tetraaoxide and the specimen was microtomed at −45°C to an ultrathin section of 70-nm thickness. The phase structure was analyzed with a TEM microscope (Hitachi HT 300).

RESULTS AND DISCUSSION

IR Studies

Figure 1 describes the IR spectra of pure DTMPTA in the region of 2000–1000 cm^{-1}. The peak positions and their respective assignments are given in Table II. These peaks are in good agreement with the literature values[32] and can be explained from the structure of DTMPTA as shown below:

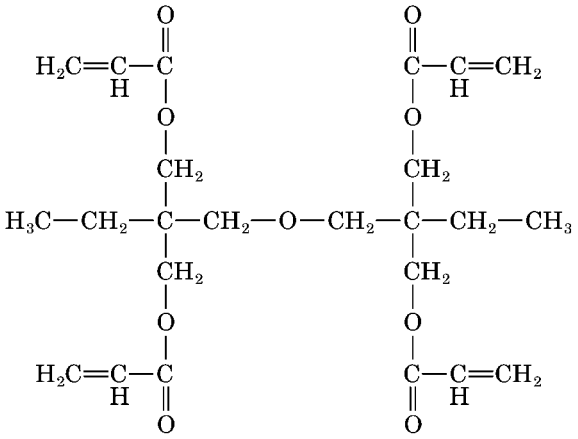

DTMPTA

The structure shows that DTMPTA is an unsaturated acrylic monomer having four unsaturations with a very bulky type of structure. In the course of irradiation it can effectively use some of its unsaturations to form huge amounts of free radicals. Mixing DTMPTA with polymers like PE or EVA can increase the crosslinking efficiency of the respective polymers by producing free radicals.[23]

DTMPTA undergoes polymerization upon irradiation through unsaturation and forms a network structure by crosslinking. As a result, it transforms from the liquid to the solid state. Ta-

Table II Peak Position and Peak Assignment for Pure DTMPTA

Wave Number (cm^{-1})	Functional Group (Mode)
1730	>C═O (carbonyl stretching)
1630	>C═C< (double bond stretching of vinylidine group)
1460	$>CH_2$ (scissor vibration)
1406	$>CH_2$ (in-plane vibration)
1275	C—H (in-plane deformation of —CH═CH_2)
1190	Asymmetric C—O stretching vibration
1120	Asymmetric C—O stretching of aliphatic ether
1060	Symmetric C—O—C stretching vibration of acrylate

Adapted from Socrates.[32]

Table III Change in DTMPTA with Irradiation

Irradiation Dose (kGy)	$\frac{A_{1730}}{A_{1460}}$	$\frac{A_{1630}}{A_{1460}}$	$\frac{A_{1408}}{A_{1460}}$	$\frac{A_{1275}}{A_{1460}}$	$\frac{A_{1190}}{A_{1460}}$	$\frac{A_{1110}}{A_{1460}}$
0	2.5	0.73	1.69	2.66	0.93	1.17
20	2.5	0.50	0.88	0.66	1.32	1.10
50	2.6	0.43	0.85	0.51	1.34	1.11
100	2.6	0.42	0.86	0.50	1.38	1.10
200	2.9	0.44	0.87	0.49	1.42	1.15
500	3.1	0.44	0.75	0.50	1.46	1.14

ble III gives the changes in the absorbances on irradiation. All the residual unsaturation observed in the crosslinked material must have been due to the unreacted double bonds (peak at 1630 cm^{-1}). The restricted mobility of the DTMPTA molecules was due to their bulky structure that shields the double bonds from further reaction in the 3-dimensional DTMPTA network formed during irradiation. At higher irradiation doses (≥200 kGy) the increase in the absorption ratio of the 1730 cm^{-1} peak with respect to 1460 cm^{-1} might be due to the oxidation at higher irradiation doses (Table III).

Figure 2 shows the IR spectra in the region of 2000–500 cm^{-1} for EVA, PE, and their 50:50 blend without irradiation. The IR spectra of pure EVA showed an absorption peak at 1730 cm^{-1} that was due to carbonyl stretching ($>$ C═O) from an ester group; at 1460 cm^{-1} due to C—H bending of $>$ CH_2; at 1370 cm^{-1} due to C—H bending of —CH_3; at 1250 cm^{-1} (split) due to C—H stretching; at 1120 cm^{-1} due to —C—O—C ether linkage; at 1023 cm^{-1} due to ═C—O—C of the ester group; at 722 cm^{-1} due to C—H rocking; and at 956 and 612 cm^{-1} due to the acetate group C—H deformation and C—O—C bending, respectively (Table IV). On the other hand, PE showed peaks at 1460, 1370, and 722 cm^{-1}. Apart from these, PE showed a very small peak at 1308 cm^{-1} that was attributable to the branch points, which was probably overlapped with the EVA peak at 1250 cm^{-1} in the blends. The 50:50 blend of these two polymers showed an IR spectra, which was additive

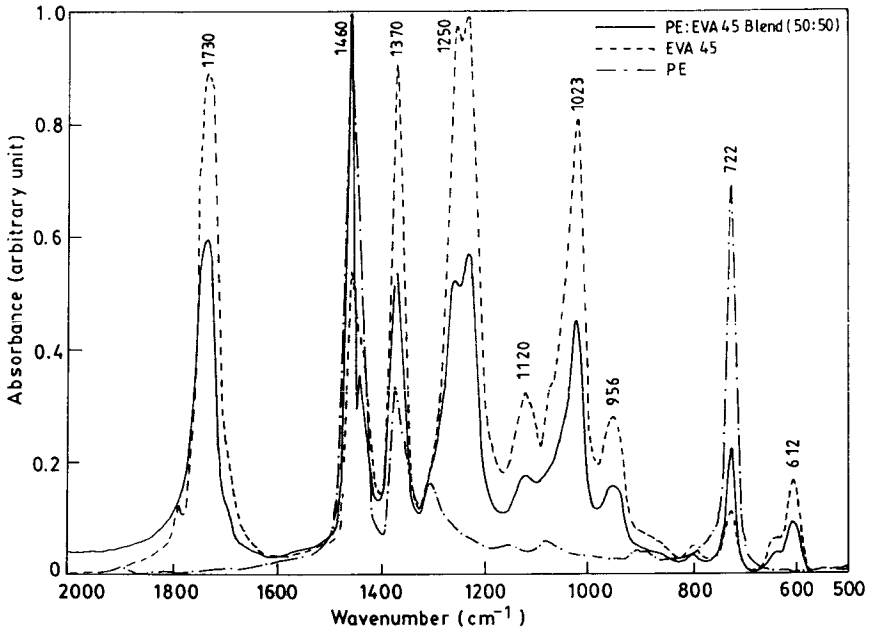

Figure 2 The IR spectra of EVA, PE, and their 50:50 blend without irradiation in the 2000–500 cm^{-1} region.

Table IV IR Peak Characterization of PE and EVA Blend

Peak (cm^{-1})	Mode of Vibration (Functional Group)
1730	>C═O stretching (ester carbonyl)
1460	$>CH_2$ scissor vibration
1370	C—H bending vibration of CH_3
1250	C—O stretching (esters and acids often split)
1120	C—O—C stretching (ether)
1023	═C—O—C stretching (ester and acids)
956	C—H deformation (acetate)
722	C—H rocking vibration (branch point of PE mainly)
612	C—O—C deformation (acetate)

Adapted from Socrates.[32]

of the constituents, indicating the individual characteristics in the blend.

Figures 3 and 4 show the IR spectra in the 2000–500 cm^{-1} region of the 50:50 blend with varying radiation doses (0–500 kGy) without DTMPTA and at a constant radiation dose of 100 kGy with varying DTMPTA levels (1–5 wt %),

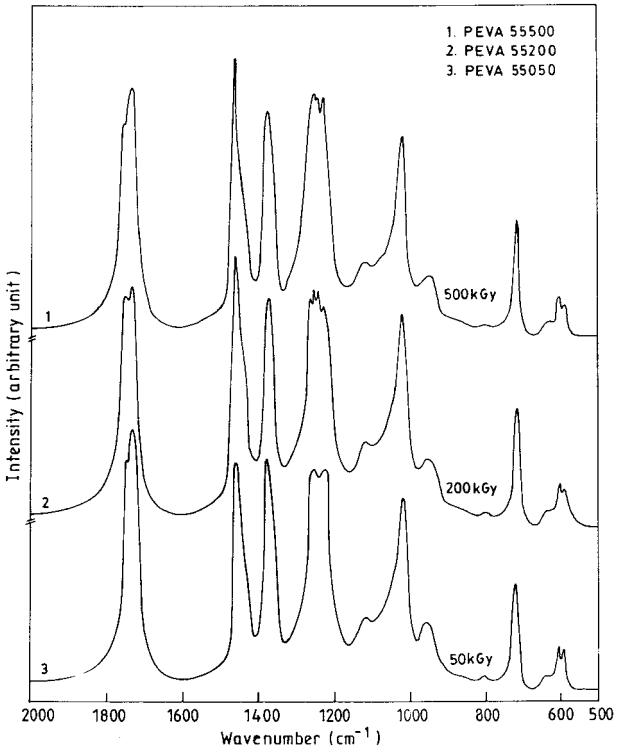

Figure 3 The IR spectra of a 50:50 PE and EVA blend with the variation in radiation dose.

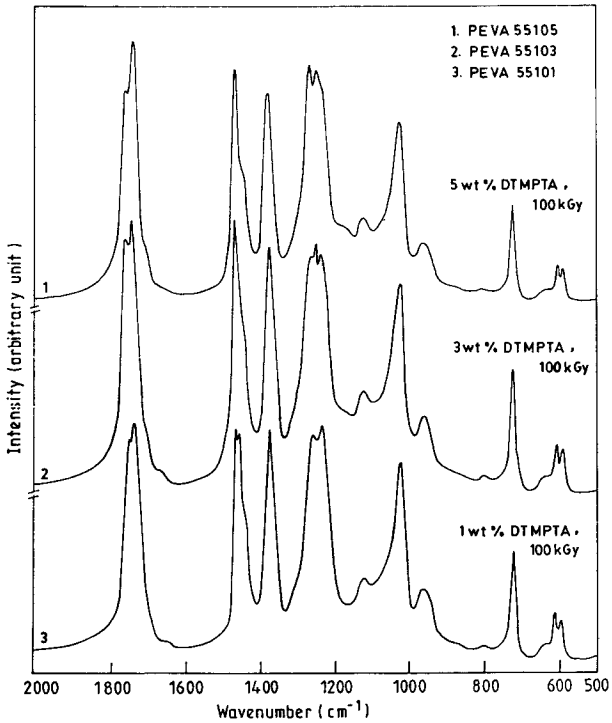

Figure 4 The IR spectra of a 50:50 PE and EVA blend at 100 kGy with the variations in the DTMPTA level.

respectively. Upon irradiation, one extra peak (compared to the unirradiated samples) appeared at 1745–1750 cm^{-1} (cyclic ketones and esters), which may have been due to the cyclization of the macroradicals formed in the process of irradiation. There was no other significant difference in the spectra when the irradiated 50:50 blend was compared with the control samples. In the blends the formation of the vinyl end groups[21–23] (peak at 1640 cm^{-1}) in PE was suppressed, possibly due to the addition of the macroradicals to the π electrons and cyclization in the presence of EVA. The unirradiated blend (50:50) with DTMPTA showed a sharp peak at around 1640 cm^{-1} (not shown) that mainly resulted from >C═C< stretching of *trans*-vinylene, which is present in DTMPTA. When the blends were irradiated, the peak at 1640 cm^{-1} disappeared. This was probably because of grafting and crosslinking of DTMPTA with PE through unsaturation.

Figure 5(a,b) shows the variation of the 1730 cm^{-1} peak due to the >C═O stretching vibration with the irradiation dose and DTMPTA level. The >C═O stretching vibration increased sharply with the radiation dose, reached its maxima at 100 kGy, followed by a sharp decrease at higher doses. The initial increase of the carbonyl

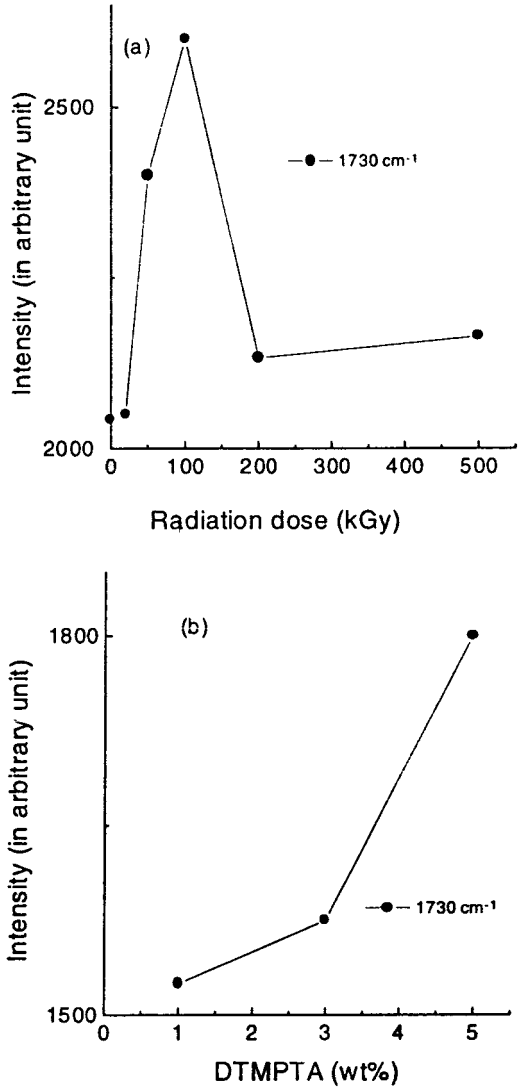

Figure 5 The variation of $>$C═O stretching of the 50:50 blend (a) with the irradiation dose without DTMPTA and (b) with DTMPTA at 100 kGy.

($>$C═O group) concentration was due to the aerial oxidation of the samples during irradiation under a normal atmosphere. As the irradiation dose increased, the probability of chain scission and degradation increased along with the oxidation and crosslinking. The decrease in carbonyl absorbance at higher irradiation doses indicated that the degradation and scission dominated among the other competitive reactions at those irradiation doses.

At constant irradiation doses the $>$C═O absorbance steadily increased with the DTMPTA level because of the presence of $>$C═O in the DTMPTA. After 3 wt % of DTMPTA, the increase in $>$C═O absorbance was sharper, indicating

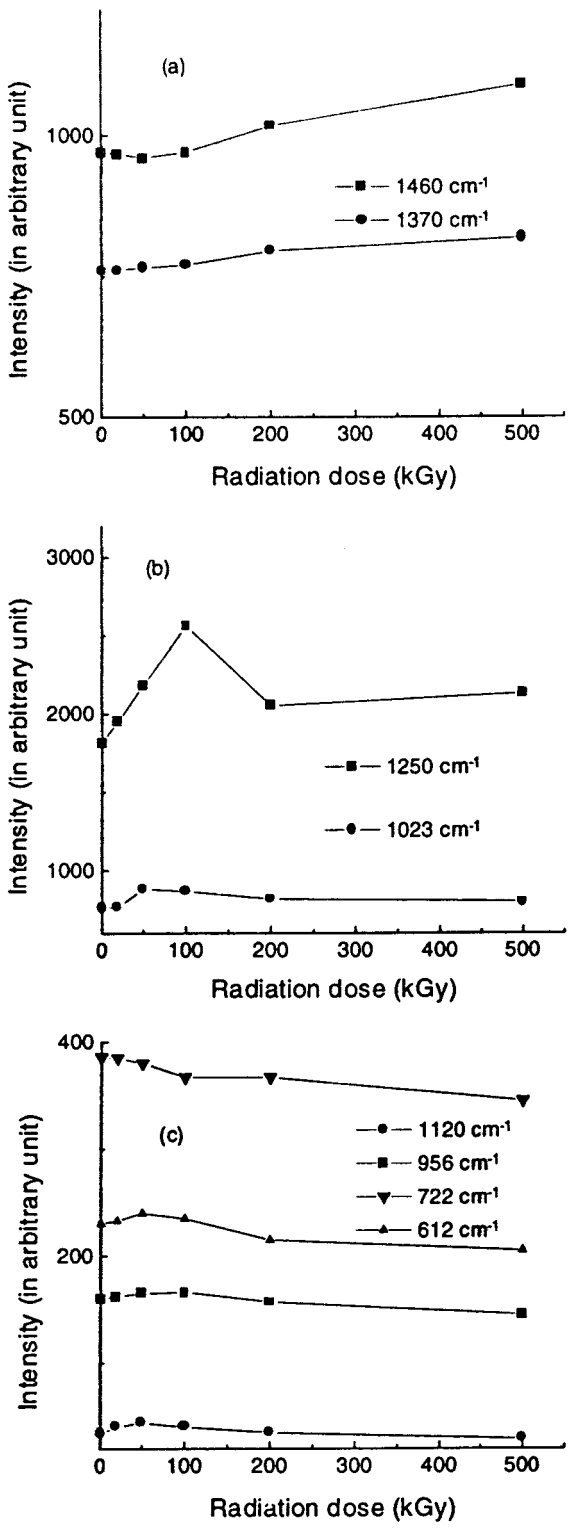

Figure 6 The plot of the absorbances of (a) the C—H stretching vibration of $>CH_2$ and $—CH_3$; (b) the C—O—C stretching vibration (ester); and (c) the C—O stretching, C—H deformation, and C—O—C deformation frequencies with the radiation dose.

that ultimately oxidation predominated in the presence of the large amount of macroradicals formed by DTMPTA.

In Figure 6(a) the absorbances (area under the peak) at 1466 and 1370 cm^{-1} are plotted against the irradiation dose. Absorption due to $>CH_2$ scissor vibration (at 1460 cm^{-1}) and $—CH_3$ bending (at 1370 cm^{-1}) remained almost constant up to 100 kGy, followed by an increase at higher irradiation doses. Up to 100 kGy there was probably a balance between various reactions (i.e., aerial oxidation, crosslinking, chain scission or disproportionation, and cyclization). After 100 kGy the chain scission by disproportionation or the cyclization reaction dominated.

The variations of absorbances at 1250 and 1023 cm^{-1} (C—O stretching and C—O—C stretching) are plotted against the irradiation dose in Figure 6(b). It is observed that the peak area around 1250 cm^{-1} increased sharply up to 100 kGy, which was followed by a decrease and then remained constant. The peak area at 1023 cm^{-1}, on the other hand, initially increased and then decreased at higher doses. These again proved that oxidation predominated up to 100 kGy and at higher doses degradation and disproportionation increased.

The absorption peak area due to acetate groups (956 and 612 cm^{-1}) remained constant up to 100 kGy [Fig. 6(c)] and was followed by a slight decrease at higher irradiation doses. This may have been due to the deacetylation of VA at higher irradiation doses. The C—O—C (ether) absorption increased at the lower irradiation doses and decreased at higher doses, which once again proved the fact that the degradation dominated only at higher irradiation doses. The same trend was observed with the peak at 722 cm^{-1} (mainly due to PE).

Figure 7(a) shows the effect of DTMPTA levels on the absorbance (areas) at 1460 and 1370 cm^{-1}, which are due to $>CH_2$ scissor vibration and C—H bending vibrations, respectively. The peak absorbance areas of $>CH_2$ scissor vibration and $—CH_3$ bending vibration remained constant up to 3 wt % of DTMPTA and was followed by an increase. Up to 3 wt % of DTMPTA there was probably a balance between different factors that persisted (e.g., addition of DTMPTA, chain scission, oxidation of the backbones of the polymers, and disproportionation or cyclization). The final increase was partly due to the contribution from DTMPTA and partly from the scission and oxidation processes.[21,23] The variation in the absorbances at 1250 and 1023 cm^{-1} supported the same trend of scission and oxidation at higher DTMPTA concentrations. The absorbance due to 724 cm^{-1} (mainly due to PE) remained constant over the whole range of DTMPTA levels, which proved that the oxidation and degradation of PE was suppressed in the presence of DTMPTA. The acetate peaks (956 and 612 cm^{-1}) remained almost constant up to 3 wt % DTMPTA, after which it slightly decreased [Fig. 7(b)]. This may have been due to the fact that at higher DTMPTA levels the deacetylation of the EVA phase takes place.

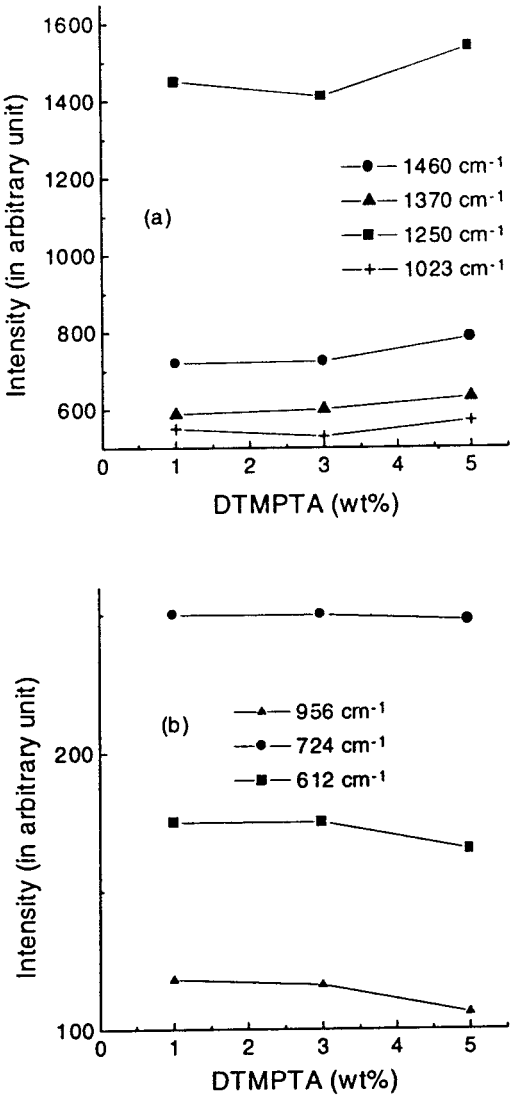

Figure 7 The plot of the absorbances (at different frequencies) with varying DTMPTA levels for (a) C—H stretching of $>CH_2$ and $—CH_3$ and C—O—C stretching (ester) and (b) C—O—C and C—H deformations.

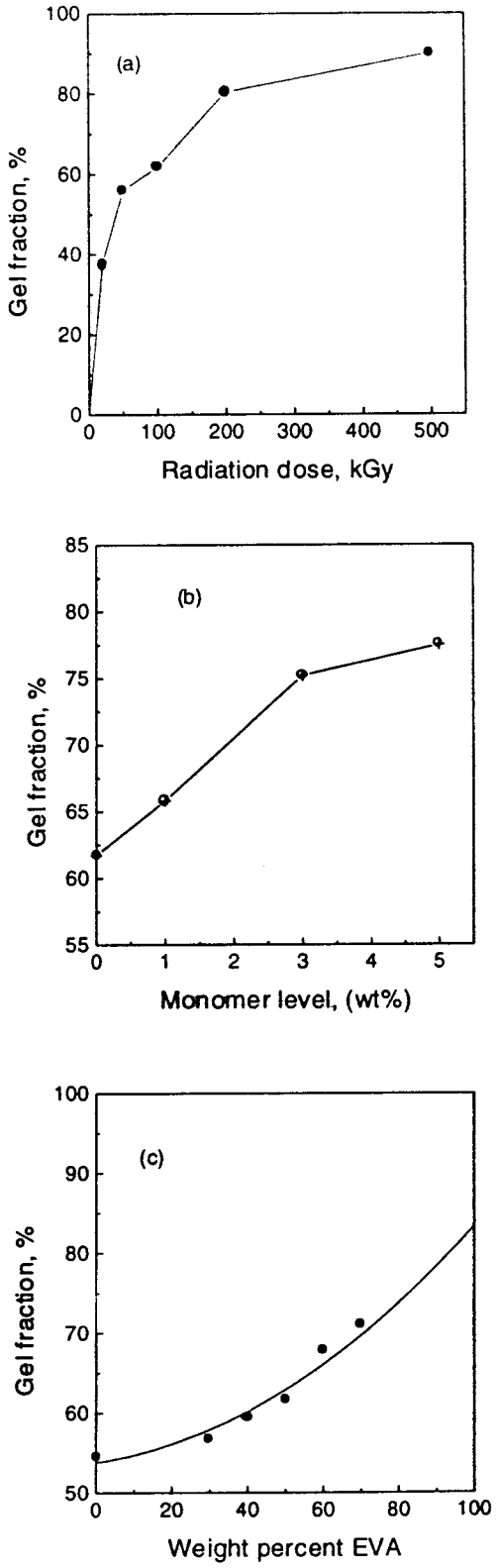

Figure 8 The gel fraction versus the (a) radiation dose for a 50:50 PE:EVA blend without DTMPTA, (b) the DTMPTA level for a 50:50 PE:EVA blend irradiated at 100 kGy, and (c) the EVA content of the blends irradiated at 100 kGy without DTMPTA.

Gel Fraction Analysis

The gel fraction values of the films are plotted against the irradiation doses [Fig. 8(a)], DTMPTA levels [Fig. 8(b)], and EVA contents of the blend [Fig. 8(c)]. For a particular blend ratio and monomer level, the gel fraction steadily increased with the radiation dose. The higher values of the gel content at higher radiation doses indicated the formation of 3-dimensional network structures. At a constant radiation dose of 100 kGy, the gel content steadily increased with the increase in DTMPTA level. The increase in the gel fraction was only marginal after 3 wt % DTMPTA concentration in the blend. At a constant irradiation dose of 100 kGy, the gel content increased with the increase in the EVA content of the blend.

At higher irradiation doses or higher concentrations of DTMPTA, a large number of radicals were formed, which would lead to a higher gel fraction by radical combinations. However, at very high doses of irradiation or DTMPTA levels, there were also possibilities of chain scission and/or degradation of the polymers. A balance was struck at optimum levels. Hence, the gel fraction did not change to a significant extent after an irradiation dose of 200 kGy and 3 wt % DTMPTA. The increase in the EVA proportion made the blend more amorphous in nature, which in turn increased its efficiency toward crosslinking at a particular radiation dose. Also, EVA can easily

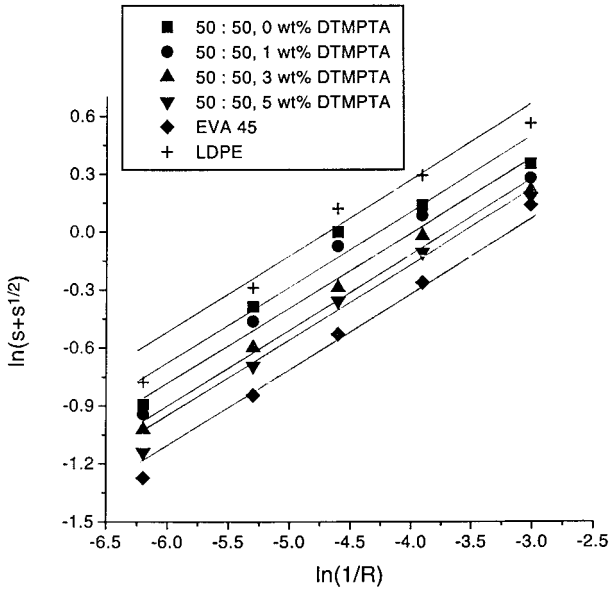

Figure 9 The plot of $\ln(s + s^{1/2})$ versus $\ln(1/R)$ for 50:50 blends with and without DMPTA, pure PE, and pure EVA.

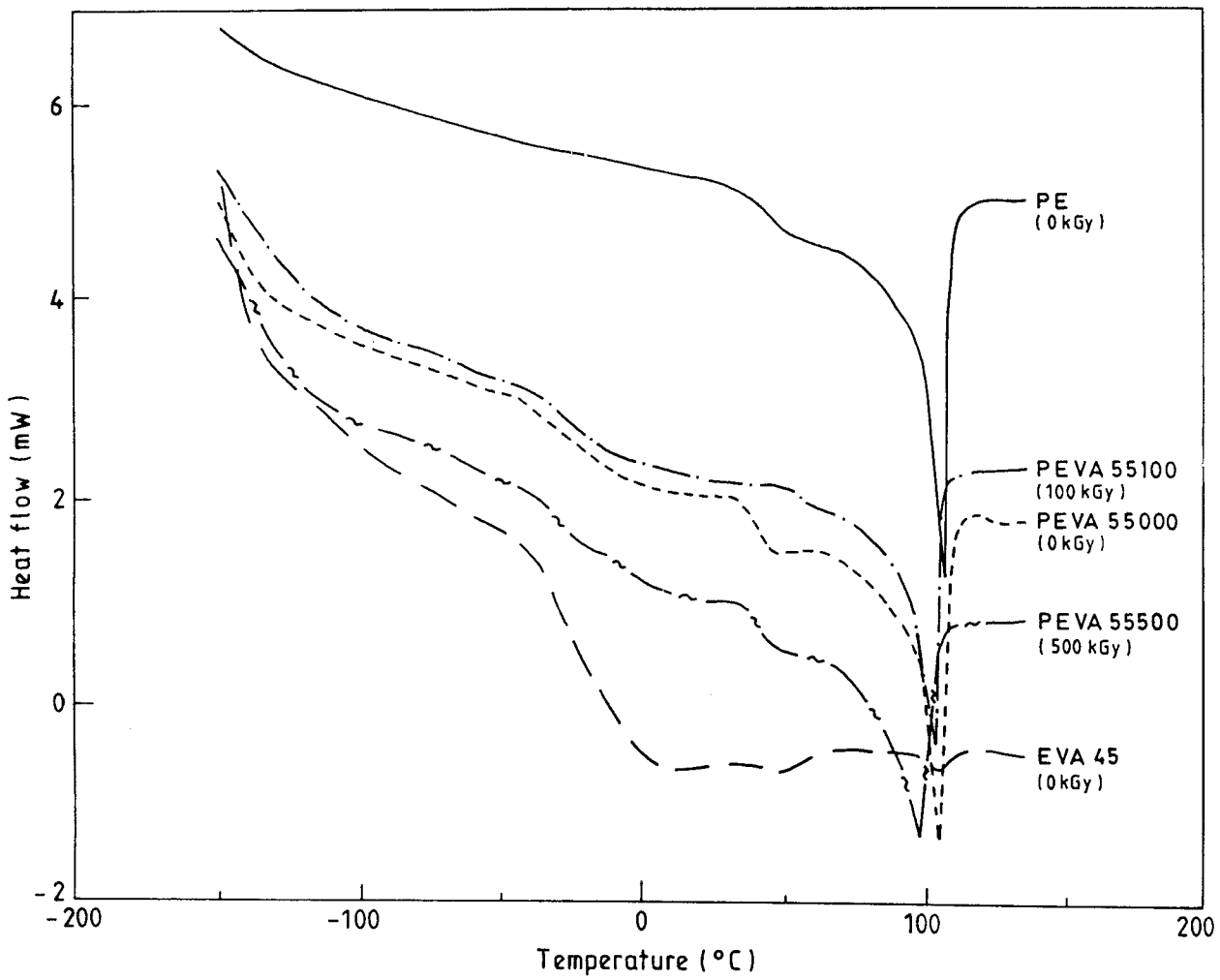

Figure 10 DSC thermograms of a 50:50 blend of pure PE and EVA irradiated at different radiation doses.

form free radicals at lower radiation doses compared to PE.[24,25]

The sol fraction (s) of a radiation crosslinked polymer can be correlated to the inverse of the irradiation dose following the Charlesby–Pinner equation[33]:

$$s + s^{1/2} = p_0/q_0 + 10/(q_0RU) \qquad (7)$$

where U is the number-average degree of polymerization, p_0 is the fracture density per unit dose (kGy^{-1}), q_0 is the density of crosslinked units per unit dose (kGy^{-1}), and R is the radiation dose (kGy). This gives an idea of the ratio of chain scission to crosslinking for the pure polymers exposed to irradiation. However, in 50:50 blend it does not give a linear correlation between ($s + s^{1/2}$) and $1/R$ as expected from the Charlesby–Pinner equation. In the blends a plot of $\ln(s + s^{1/2})$ versus $\ln(1/R)$ was made (Fig. 9). Parallel lines were drawn according to the following equation:

$$\ln(s + s^{1/2}) = 0.4 \ln(1/R) + A \qquad (8)$$

where A is a constant that depends on the blend compositions. The values of A were calculated to be 1.62, 1.54, 1.46, and 1.44 for the 50:50 blends containing 0, 1, 3, and 5 wt % of DTMPTA, respectively. The A values were calculated by a linear regression method with an average standard deviation and correlation factor of <0.15 and >0.98, respectively. It is obvious from Figure 9 that as the DTMPTA concentration increased the curve approached linearity and behaved more like pure EVA. The PE, on the other hand, did not give a linear correlation. The 50:50 blend without

Table V Results of X-Ray and DSC Studies

	X-Ray Studies				DSC Studies		
Sample Code	Crystallinity (%)	P (Å)	r (Å)	d (Å)	Crystallinity (%)	T_m (°C)	T_β (°C)
PEVA55000	23	182	5.25	4.2	27	106	−22
PEVA55020	23	178	5.25	4.20	26	106	−20
PEVA55050	23	178	5.21	4.17	26	105	−20
PEVA55100	23	176	5.25	4.20	26	104	−20
PEVA55200	21	174	5.25	4.20	24	102	−19
PEVA55500	20	162	5.29	4.24	21	99	−18
PEVA55101	22	176	5.25	4.20	26	104	−20
PEVA55103	21	174	5.21	4.17	25	103	−21
PEVA55105	20	158	5.25	4.20	24	102	−16
EVA100	—	—	—	—	—	—	−20
PEVA37000	16	178	5.25	4.2	17	104	−23
PEVA37100	16	176	5.25	4.20	16	104	−22
PEVA46100	18	176	5.25	4.20	19	104	−23
PEVA64100	26	176	5.25	4.20	28	104	−20
PEVA73000	33	178	5.25	4.20	35	105	−20
PEVA73100	32	178	5.25	4.22	34	104	−15
PE100	45	190	5.21	4.17	50	106	—

DTMPTA showed behavior similar to PE. Hence, with the increase in DTMPTA level the extent of crosslinking increased, although at higher DTMPTA levels oxidation and chain scission also increased. Similarly, with the increase in the EVA proportion of the blend the nature of the curves approached the nature of pure EVA (not shown).

DSC Studies

The DSC thermogram in Figure 10 exhibits the plots of heat flow versus temperature. Pure EVA showed two distinct transitions termed β and γ, where the γ- and β-relaxation peaks appeared at a temperature of around −135 to −130°C and around −20°C, respectively. The γ transition is associated with the crankshaft motion of the polymethylene groups of the main chain backbone. The β relaxation is associated with the branch points containing the side group (VA). The β peak becomes prominent if the concentration of the side groups exceeds a certain limit.[34]

On the other hand, pure PE exhibited one prominent endothermic peak due to the crystalline melting at around 105°C. However, the γ-relaxation peak of pure PE was not detected clearly. This may have been due to interference from the crystalline zone.[35]

Upon blending the characteristic relaxation of the individual transitions was not changed significantly, indicating the immiscible character of the blend. The γ relaxation was not changed significantly with the variation in irradiation dose, DTMPTA level, or blend variation.

The melting temperature (T_m) remained constant up to 100 kGy, and it dropped to 99°C at 500 kGy. The DSC results also supported that the percentage of crystallinity remained constant in the initial stage with the increase of radiation dose (up to 100 kGy). A further increase in the radiation dose resulted in a decrease in the percentage of crystallinity, which was also reflected in the decrease in the T_m (Table V).

The β-transition temperature (due to EVA) first increased as the films were irradiated (compared to the control sample) and remained constant up to 100 kGy. At higher radiation doses ($\geq$200 kGy), the β-transition temperature (T_β) increased (−18°C at 500 kGy). The increase in T_β at higher radiation doses may have been attributable to a decrease of the segmental mobility as a result of the formation of 3-dimensional network structures.

Similarly, the T_m and the T_β both shifted to higher temperatures with the increase in the DTMPTA level of the blends.

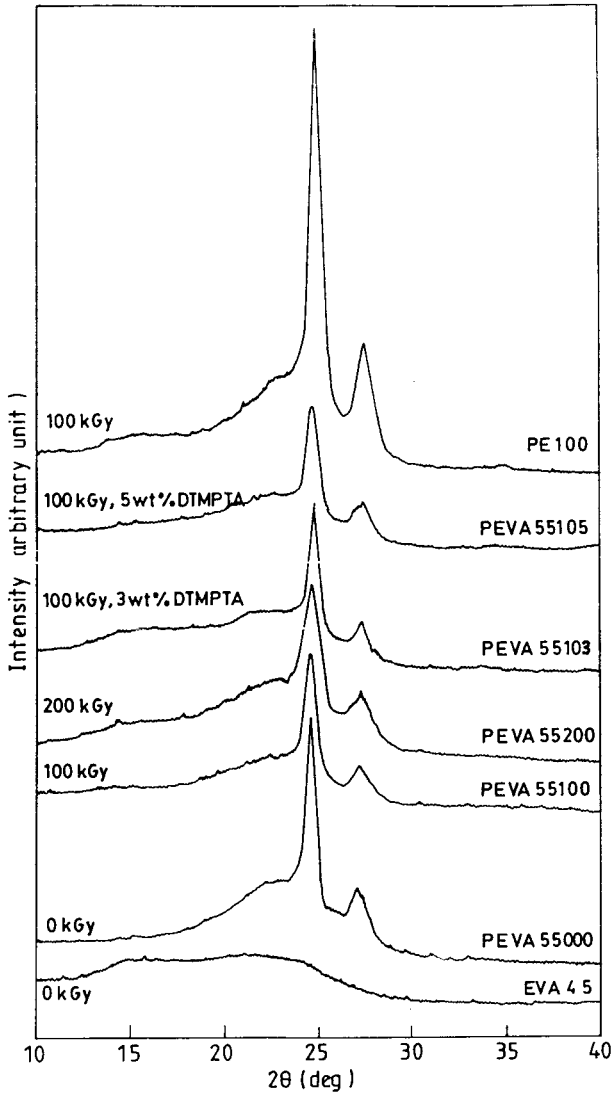

Figure 11 The X-ray diffraction pattern of 50:50 blends with and without DTMPTA, PE, and EVA.

X-Ray Studies

Figure 11 shows the XRD patterns of the control film, the 50:50 blend of PE and EVA irradiated at different radiation doses, and pristine PE and EVA samples irradiated at 100 kGy. There were mainly two crystalline peaks in the diffraction patterns of the blends, one in the angular range (θ) of 12.2–12.4° and another between 13.6 and 13.8°. The diffraction angles corresponded to an orthorhombic unit cell. These peaks are well characterized in PE and correspond to specific crystallographic planes 110 and 200 (Miller Indices). On the other hand, EVA contributes only to the amorphous portion in the blend.[30]

The crystallite size, interchain distance, and interplanar distance were calculated with respect to the peak in the 12.2–12.4° angular range. It was observed that the crystalline peaks were distinctly broadened (crystallite size decreased) at higher radiation doses and higher concentrations of DTMPTA. This was due to the destruction of the crystallite portions during crosslinking at those irradiation doses and DTMPTA levels. The percentage of crystallinity remained more or less constant up to 100 kGy and decreased at higher radiation doses. Interplanar and interchain distances remained constant because the angle of the peak (θ) did not vary significantly, despite the variation of the irradiation doses, DTMPTA levels, or blend ratio.

For the 50:50 blend films irradiated at 100 kGy, the minimum crystallinity was obtained for the samples containing 5 wt % of DTMPTA. This was probably due to the efficient crosslinking at higher DTMPTA levels. The crystallite size also followed the same trend.

No significant change in the crystallite size, interchain distance, or interplanar distance was observed with the variation in the blend ratio. The percentage of crystallinity was systematically increased with the increase in PE content of the blend.

Microscopy Studies

Figure 12(a–c) shows the morphology of PEVA73000, PEVA55000, and PEVA37000. The black domains indicate the positions of the extracted EVA phase. In the PE-rich blend PEVA7300, which had 30 wt % of EVA, PE was found as the continuous matrix. Figure 12(b) indicates the morphology of PEVA55000, which reveals the fine dispersion of EVA phases in the continuous matrix of PE. AFM and TEM studies also confirmed the morphology of the 50:50 blends [Fig. 12(d,e)]. The domain size of EVA was in the range of 1–2 μm. A cocontinuous morphology was observed for the PEVA37000 blend with spherical, elliptical, and elongated elliptical domains. This variation in the domain morphology can be explained.

The molten polymeric materials during melt mixing experience a high shearing action. The induced shearing force deforms the dispersed molten polymer into elongated, rodlike particles, which progressively constrict until rupture. When the particles come out of the shearing zone, they may fully or partly relax to regain their original spherical, elliptical, or elongated elliptical shapes and may remain isolated from each other. How-

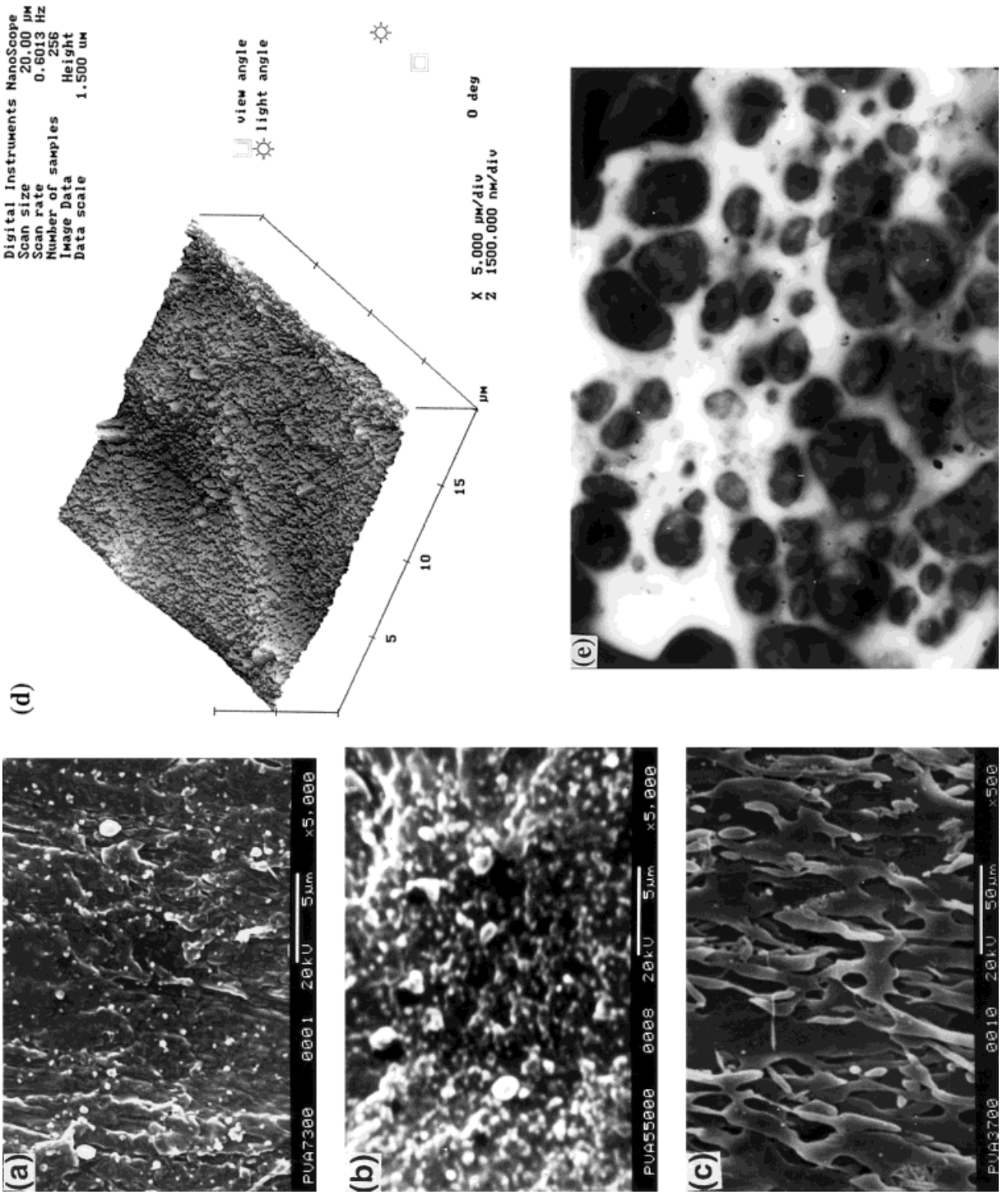

Figure 12 SEM photomicrographs of toluene etched samples with varying blend proportions without irradiation: (a) 70:30, (b) 50:50, and (c) 30:70 PE:EVA. (d) The AFM topography of a 50:50 PE:EVA blend. (e) A TEM photomicrograph of a 50:50 PE:EVA blend (original magnification ×4000).

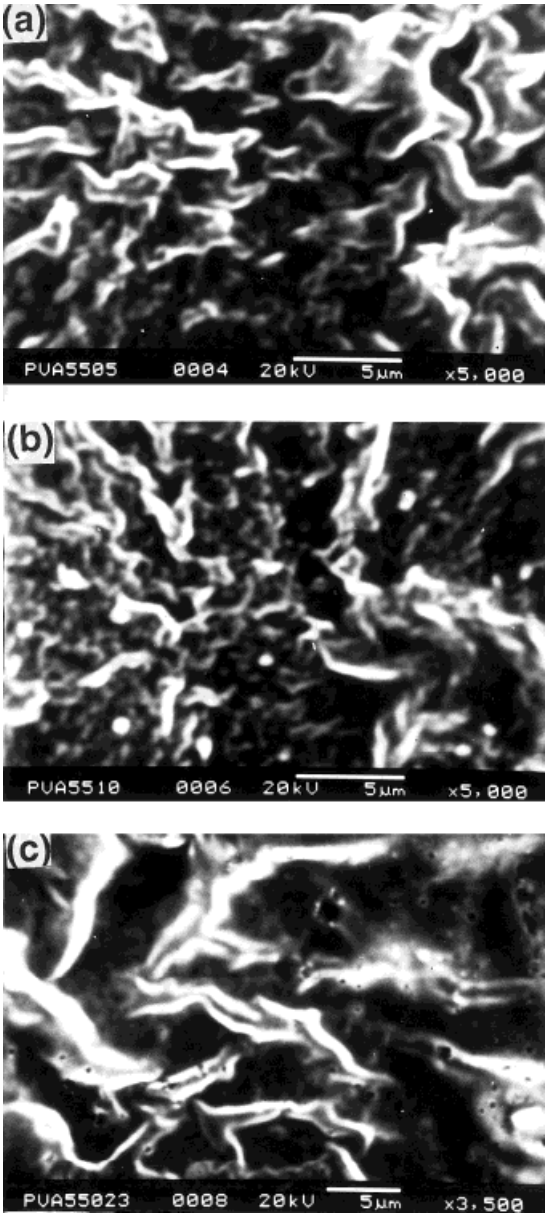

Figure 13 SEM photomicrographs of nitric acid (concentrated) etched samples of (a) PEVA55050, (b) PEVA55100, and (c) PEVA55023.

ever, there is also a tendency for particle recombination, leading to intricate shapes. The two components of the blends (PE and EVA45) have different polarities and melt viscosities. Thus, an immiscible blend morphology is expected. Because of the high melt flow index or low melt viscosity of PE, the blends preferentially have a PE continuous matrix, even at a higher proportion of EVA.

Figure 13(a,b) shows the SEM photomicrographs of 50:50 blends irradiated at 50 and 100 kGy, which were etched with concentrated nitric acid to extract the EVA phase. The morphology did not change: dispersed EVA particles were found in the PE matrix. However, the shape of the particles changed. Figure 13(c) shows the SEM photomicrograph of a 50:50 blend irradiated at 20 kGy containing 3 wt % of DTMPTA. DTMPTA is a polar monomer, which can plasticize the EVA phase. This gave rise to a cocontinuous morphology of this blend in which both phases interpenetrated each other.[14]

CONCLUSIONS

EVA-LDPE films crosslinked to varying degree by irradiation and DTMPTA were characterized by IR spectroscopy, gel fraction, XRD, DSC, and morphology. The following conclusions were drawn.

1. Oxidation and crosslinking dominate up to a 100-kGy irradiation dose, after which the scission and disproportionation become the major mechanism in the 50:50 PE and EVA blends without DTMPTA. At a constant irradiation dose the deacetylation is suppressed due to the addition of DTMPTA in the blend. After 3 wt % of DTMPTA chain scission becomes the progressively dominating process.
2. The gel fraction of the films increases with the increase in irradiation dose, DTMPTA level, and EVA content of the blend. The sol fraction of the control and the blend with and without DTMPTA fit into the modified type of Charlesby–Pinner equation.
3. The XRD and DSC studies reveal that the crystalline portion of the blends is affected by irradiation only at higher radiation doses (200 kGy and above).
4. SEM studies show that the PE forms the continuous matrix in the 50:50 blend; however, a cocontinuous structure is observed in the 30:70 blend of PE and EVA. The morphology does not change after irradiation. However, the addition of 3 wt % DTMPTA causes the blend to form a cocontinuous morphology.

The authors are grateful to Dr. A. B. Majali and Dr. S. Sabharwal, Radiation Processing Section, Bhabha Atomic Research Centre, Mumbai, for funding this

project and for the experimental assistance with the radiation processing.

REFERENCES

1. Bhowmick, A. K.; Mangaraj, D. In Rubber Products Manufacturing Technology; Bhowmick, A. K., Hall, M. M., Benary, H., Eds.; Marcel Dekker: New York, 1994; p 119.
2. Clegg, D. W.; Collyer, A. A. Irradiation Effects on Polymers; Elsevier: New York, 1991.
3. Clough, R. In Encyclopedia of Polymer Science and Technology; Wiley: New York, 1989; Vol. 15, p 666.
4. McGinnis, V. D. In Encyclopedia of Polymer Science and Technology; Wiley: New York, 1986; Vol. 4, p 421.
5. Dworjanyn, P. A.; Garnet, J. A.; Khan, M. A.; Maojun, X. Y.; Ring, M. G.; Nho, C. Y. Radiat Phys Chem 1994, 42, 31.
6. Charlesby, A. Atomic Radiation and Polymers; Pergamon: London, 1960.
7. Chaprio, A. Radiation Chemistry of Polymeric Systems; Interscience: New York, 1962.
8. Dole, M. The Radiation Chemistry of Macromolecules, I; Academic: New York, 1972.
9. Wiesner, L. Radiat Phys Chem 1984, 22, 587.
10. Mullins, L. Rubber Dev 1978, 31, 92.
11. Fisher, W. K. U.S. Pat. 3,835,201, 1972.
12. Elliott, D. J. Nat Rubber Technol 1981, 12, 59.
13. Campbell, D. S.; Elliott, D. J.; Wheelans, M. A. Nat Rubber Technol 1978, 9, 21.
14. Chowdhury, N. R.; Bhowmick, A. K. J Appl Polym Sci 1989, 38, 1091.
15. Jha, A.; Bhowmick, A. K. Rubber Chem Technol 1997, 70, 798.
16. Aoshima, M.; Jinno, T.; Sassa, T. Kautsch Gummi Kunst 1992, 45, 644.
17. Banik, I.; Bhowmick, A. K. Radiat Phys Chem 1999, 54, 135.
18. Bohm, G. G. A.; Teekrem, J. O. Rubber Chem Technol 1982, 55, 575.
19. Sen Majumdar, P.; Bhowmick, A. K. Radiat Phys Chem 1998, 53, 63.
20. Nethsinghe, L. P.; Gilbert, M. Polymer 1988, 29, 1935.
21. Chaki, T. K.; Roy, S.; Despande, R. S.; Majali, A. B.; Tikku, V. K.; Bhowmick, A. K. J Appl Polym Sci 1994, 53, 141.
22. Chaki, T. K.; Roy, D.; Majali, A. B.; Tikku, V. K.; Bhowmick, A. K. J Polym Eng 1994, 13, 17.
23. Datta, S. K.; Bhowmick, A. K.; Thripathy, D. K.; Chaki, T. K. J Appl Polym Sci 1996, 60, 1329.
24. Martinez-Padro, M. E.; Vera-Graziano, R. Radiat Phys Chem 1995, 45, 93.
25. Abdel-Bary, E. M.; El-naser, E. M. Radiat Phys Chem 1996, 48, 689.
26. Harnischfiger, P.; Knizel, P.; Jungnickel, B. J. Angew Makromol Chem 1990, 175, 157.
27. Mateev, M.; Karageorgier, S. Radiat Phys Chem 1998, 31, 205.
28. Chattopadhyay, S.; Chaki, T. K.; Bhowmick, A. K. J Appl Polym Sci 2001, 79, 1877.
29. Chattopadhyay, S.; Chaki, T. K.; Bhowmick, A. K. Radiat Phys Chem 2000, 59, 501.
30. Alexander, L. E. X-Ray Diffraction Methods in Polymer Science; Wiley–Interscience: New York, 1969.
31. Kemp, G. Polymer Characterization; Hanser: New York, 1980.
32. Socrates, G. Infrared Characteristic Group Frequencies; Wiley–Interscience: New York, 1980.
33. Charlesby, A.; Pinner, S. H. Proc R Soc 1959, A249, 367.
34. Oakes, W. G.; Robinson, D. W. J Polym Sci 1954, 14, 505.
35. Koleske, J. V.; Lundberg, R. D. J Polym Sci, Polym Phys Ed 1969, 7, 795.